COMMUNICATION

Flexible Electronics

**ADVANCED
MATERIALS
INTERFACES**

www.advmatinterfaces.de

Bias-Induced Electrochemical Electron Doping of Organic Semiconductor Contacts

Chao Zhao, Adrian Nugraha Utama, Kim-Kian Choo, Lay-Lay Chua, Rui-Qi Png,* and Peter K. H. Ho

It is well-known that thin polyethylenimine and polyethylenimine (ethoxylated) (PEIE) layers can reduce the work function of metals, metal oxides, and conducting polymers by 1 eV or more through an interface dipole, but this is not generally sufficient to produce an ohmic electron contact. Here, it is shown that a short, positive-bias preconditioning can switch the injection characteristics of a self-assembled monolayer of PEIE on poly(3,4-ethylene dioxythiophene):poly(styrenesulfonic acid) (PEDT:PSSH) from electron-blocking to electron-injecting into poly(N,N'-bis(2-octyldodecyl)-1,4,5,8-naphthalenebis(dicarboxy-imide)-2,6-diyl)-*alt*-(2,2′-bithiophene)-5,5′-diyl). Despite its low work function (4.0 eV) and favorable energy level alignment, the PEIE-modified contact is initially blocking because the tunneling barrier limits carrier accumulation. The prebias boosts this accumulation density through an interfacial solid-state electrochemical process that positively charges the PEIE, which induces charge compensation by mobile electron carriers in the adjacent semiconductor layer through the field effect. This mechanism to trigger the ohmic transition appears to be general, as similar effects, albeit to a small extent, is found in semiconductors with even smaller electron affinity. This is the first example of ohmic electron injection from PEDT:PSSH into an organic semiconductor, which would be useful for fabricating tandem and other cells.

Achieving ohmic contacts is key to maximizing power efficiency, and operational stability, of organic semiconductor (OSC) devices, including organic light-emitting diodes, field-effect transistors, and solar cells. In general, this requires the accumulation of sufficient carrier density in a so-called δ-doped layer at the semiconductor side of the contact.[1] The conventional approach for this is to employ electrodes with sufficiently high, or low, work function to match the ionization energy (I_E), or electron affinity (E_A), respectively, of the OSC. The precise work function required depends on the injection resistance that can be tolerated, but the threshold for ohmic transition lies well beyond the onset of Fermi level pinning.[2] For making hole contacts, air stable hole-doped conducting polymers with work functions of up to 5.2 eV, such as poly(3,4-ethylenedioxythiophene):poly(styrenesulfonic acid) (PEDT:PSSH)[3] and sulfonated poly(thiophene-3-[2-(2-methoxyethoxy)ethoxy]-2,5-diyl):poly(4-hydroxystyrene) (S-P3MEET:PHOST)[4] have long been available. For making electron contacts, however, stable electron-doped conducting polymers with work functions smaller than ≈4.0 eV are not available because of vulnerability to oxygen reduction reaction.[5] Various schemes have thus been devised to fabricate electron-doped semiconductor electron transport/injection layers,[6] including the use of multivalent anions as latent electron donors[7] with the self-compensated polymer platform which allow heavily doped conducting polymers to be obtained over a wide range of work functions, free from the problem of "dopant migration."[8] The ability to make ohmic contacts at will, in particular to the more challenging high I_E and low E_A semiconductors, is important for continued advancement in the field.

Recently, polyethylenimine (PEI), polyethylenimine (ethoxylated) (PEIE), and related polymers, and even amine solvents,[9] have been suggested to greatly improve electron injection when applied to various surfaces, including metals, metal oxides, and PEDT:PSSH.[10] However, PEI and PEIE are both electronic insulators, so this result is puzzling. Careful recent work has shown that their thin interlayers indeed act as tunnel barriers, not ohmic electron contacts; they confine holes injected from the opposite contact to induce an electric-field realignment improving electron injection, but far away from ohmic regime.[11] This mechanism is the same as that demonstrated some time ago through the use of layer-by-layer assembled monolayers to confine carriers in organic light-emitting diodes.[12,13] The large 1 eV work-function reduction generated by the PEI or PEIE interlayers is thus essentially futile. Their electron contacts are nonohmic, despite their low work functions.[14] This is not surprising. It has been well-established

Dr. C. Zhao, A. N. Utama, Dr. R.-Q. Png, Prof. P. K. H. Ho
Department of Physics
National University of Singapore
Lower Kent Ridge Road, Singapore S117550, Singapore
E-mail: phypngrq@nus.edu.sg
Dr. K.-K. Choo, Prof. L.-L. Chua
Department of Chemistry
National University of Singapore
Lower Kent Ridge Road, Singapore S117552, Singapore

The ORCID identification number(s) for the author(s) of this article can be found under https://doi.org/10.1002/admi.201900607.

that even if the thermodynamic component of the barrier can be made to vanish through dipolar dielectric layers, the kinetic barrier remaining due to the insulating interlayer can generally prevent the contact from becoming ohmic.[15] Yet, organic solar cells, which are particularly sensitive to contact resistance do show improvements.[16] We attribute this curious situation to transient electron doping of the contact by photoinduced electron transfer from the amine lone pair in PEI or PEIE to the photohole in the semiconductor when exposed to light. Photoinduced electron transfer from organic dyes to tertiary amines has been very well established.[17] Nevertheless, there are also sporadic reports of good electron injection through PEI/PEIE interlayers,[18] and recently, in thicker blend films of PEIE with ω-trialkylammonium-functionalized polyfluorene.[19] Some literature suggests impurities,[20] or the PEIE itself, can lightly n-dope the OSC and passivated electron traps.[21] Therefore, whether PEIE can provide ohmic electron contact in the dark is controversial.

Here, we provide unequivocal evidence using a well-defined system where a molecularly thick PEIE monolayer is self-assembled on PEDT:PSSH that despite its favorable work function (4.0 eV) and energy-level alignment with a diagnostic organic semiconductor, poly(N,N'-bis(2-octyldodecyl)-1,4,5,8-naphthalenebis(dicarboxy-imide)-2,6-diyl)-alt-(2,2'-bithiophene)-5,5'-diyl) (PNDI), with matching E_A (3.9 eV), the contact is blocking, and becomes injecting only when preconditioned by a short positive bias. This generates an electron-doped contact in-device at the PNDI interface with PEIE, producing an electron injection contact, in the dark, without requiring photoinduced electron transfer. The mechanism is an interfacial solid-state electrochemistry in which charging of the PEIE interlayer by hole injection amplifies the accumulation of electrons on the OSC side through an electric field effect. While multivalent anions can act as powerful latent electron donors when dispersed as small ion clusters in polymer matrix for the generation of electron injection contacts in the absence of air and moisture,[7] such in-device electrochemistry provides a useful alternative approach. The significance of this result, beyond resolving a longstanding controversy, is its clear path toward

the design of interlayers for in-device formation of electron-doped (and by corollary, hole-doped) interfaces through bias preconditioning.

We prepared the self-assembled PEIE overlayers on both PEDT:PSSH, and indium-tin oxide (ITO), surfaces (see **Figure 1**a for chemical structures). ITO substrates are cleaned by O$_2$-plasma treatment, and PEDT:PSSH films are spin-cast (50 nm thick) from a commercial PEDT:PSSH solution purified by dialysis, and then baked at 150 °C.[22,23] In a typical PEIE assembly, a commercial PEIE solution is diluted with 2-methoxyethanol to 0.4 wt%, spin-cast to a thin overlayer, the film then spin-rinsed with 2-methoxyethanol to remove unbound polymer, and baked at 100 °C, an extension of the well-known polyelectrolyte assembly method.[13] X-ray photoemission spectroscopy (XPS) shows most of the PEIE overlayer is bound, and cannot be removed by the spin-rinse step (on ITO: see Figure S1a–c; on PEDT:PSSH, Figure S1d–f in the Supporting Information). The thickness of this self-limiting overlayer is 1 nm on ITO, and 4 nm on PEDT:PSSH (mixed PSSH:PEIE frontier layer), based on XPS core-level photoemission attenuation analysis.

This self-assembled PEIE monolayer is sufficient to give an eV-scale reduction in the work function of both PEDT:PSSH and ITO surfaces. Figure 1b shows the low-energy cutoff (LECO) and the valence band (VB) edge regions of PEDT:PSSH/PEIE and ITO/PEIE assemblies, measured by ultraviolet photoemission spectroscopy (UPS). The vacuum work function φ_{vac} obtained in the usual way from the difference in photoelectron kinetic energies between LECO and Fermi level (FL): $\varphi = KE_{LECO} - KE_{FL} + h\nu$, where $h\nu$ is He I photon energy (21.21 eV) shows a large reduction from 5.2 to 3.9 eV and 4.8 to 4.0 eV, after PEIE assembly on PEDT:PSSH and ITO, respectively. Devices are then fabricated with 120 nm thick spin-cast PNDI as diagnostic OSC, and evaporated Al as top contact, to define eight 4.3 mm^2 devices for evaluation of the internal effective work functions, and electron injection characteristics. PNDI is an important n-type polymer with high electron mobility and deep lowest-unoccupied molecular orbital (LUMO).[24,25]
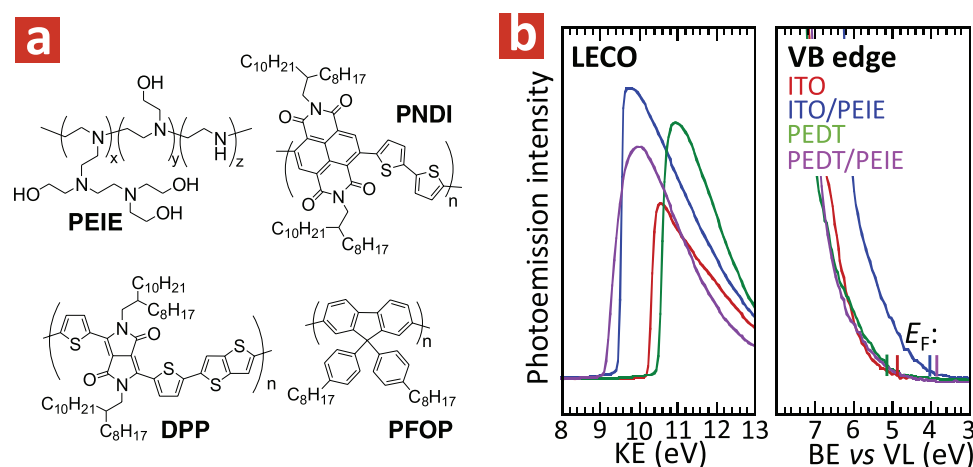
Figure 1. Chemical structures and solid-state ultraviolet photoemission spectroscopy. a) Chemical structure of materials used in this study. b) UPS spectra of ITO substrate, PEDT:PSSH film, ITO/PEIE, and PEDT:PSSH/PEIE, showing the low-energy cutoff (LECO) and valence band (VB) edge regions. The Fermi energy (E_F) of each film is marked.

The low work-function PEDT:PSSH/PEIE surface persists substantially unchanged in the completed device. To check this, we employed electroabsorption spectroscopy (EA) to measure the diode built-in potential V_{bi} through the quadratic Stark effect.[26] The V_{bi} is given by: $V_{bi} = \varphi_{el2} - \varphi_{el1}$, where φ_{el2} and φ_{el1} are the effective work functions of the two electrodes ($\varphi_{el2} > \varphi_{el1}$), each measured relative to the hypothetical internal vacuum level (VL) of the semiconductor.[26] The PEDT:PSSH/PNDI/Al diode gives inversion of the Stark peak at $V_{dc} = 1.3$ (±0.05) V, which indicates $V_{bi} = 1.3$ V (**Figure 2**a). The φ_{el} of Al on non FL-pinning polymer organic semiconductors is 3.4 eV.[26] This is considerably shallower than the E_A of PNDI. So electron transfer to the semiconductor LUMO band edge to give FL pinning can be expected.[27] The estimated energy-level alignment diagram is shown in inset of Figure 2c. Assuming the PNDI/Al contact is pinned at 4.05 eV (UPS gives 4.1 eV),[28] the vacuum level offset ($\Delta = 4.05 - 3.4 = 0.65$ eV) corresponds to a sizeable accumulation of electron density, which can be expected to drive up φ_{el} of PEDT:PSSH in the device.[29] For comparison, the PEDT:PSSH/PEIE/PNDI/Al diode gives $V_{bi} = 0.05$ (±0.05) V (Figure 2b). Assuming $\varphi_{el,Al}$ is unchanged, φ_{el} of the

PEDT:PSSH/PEIE/PNDI contact is 4.1 eV (inset, Figure 2d). This provides an electron-only device with nearly symmetric electron injection barriers. Thus the effective work function of PEDT:PSSH/PEIE in the device is practically identical to its vacuum work function.

Despite its work function matching E_A of PNDI, the PEDT:PSSH/PEIE contact does not inject electrons, so the work function improvement is futile. The JV characteristic of the PEDT:PSSH/PNDI/Al diode shows strong electron injection from Al in forward bias, but not hole injection from Al, nor electron injection from PEDT:PSSH, in reverse bias (Figure 2c). On the other hand, the PEDT:PSSH/PEIE/PNDI/Al diode in the first cycle sweep ($0 \rightarrow +8 \rightarrow -8 \rightarrow 0$ V) shows strong electron injection only from Al, but not PEDT:PSSH/PEIE (Figure 2d). It was demonstrated by Steyrleuthner et al. that contacts like Ba, Ca with low work functions do not form ohmic electron contacts to this material.[30] Later on, it was found by Wetzelaer et al. that Cs_2CO_3 does form an ohmic contact, probably due to doping.[25] It is still not really understood why many conventional cathodes do not work for PNDI. However, we found here that Al can surprisingly make ohmic contact
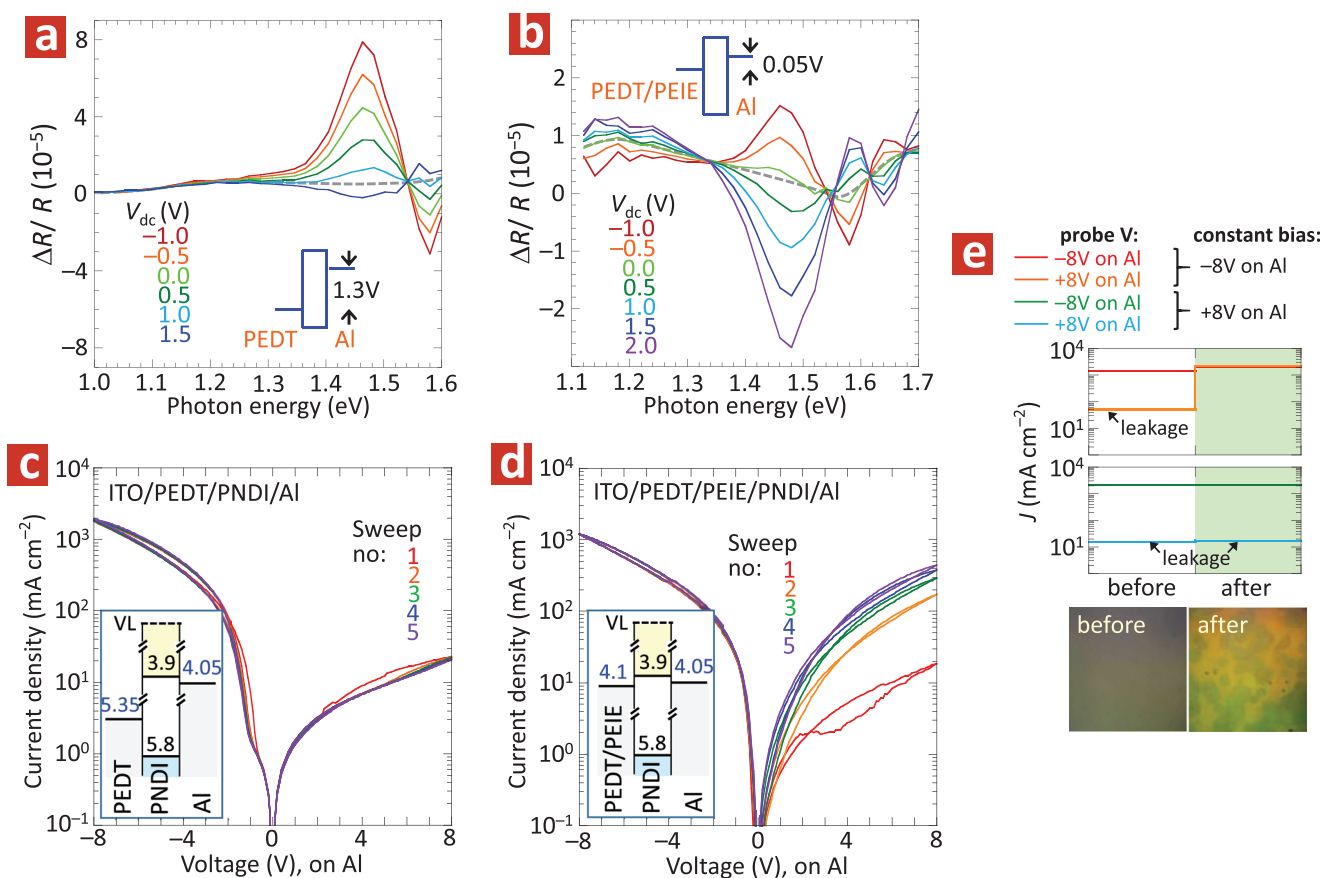
Figure 2. Device spectroscopy and current–voltage (JV) measurements. Electroabsorption spectroscopy at different dc biases V_{dc} for: a) ITO/PEDT:PSSH/PNDI/Al and b) ITO/PEDT:PSSH/PEIE/PNDI/Al devices. Temperature, 30 K; modulation frequency, 535 Hz; ac amplitude, 0.5 V_{rms}. EA was performed at 30 K to avoid bulk carrier injection. Diode V_{bi} is shown in inset. JV characteristics for: c) ITO/PEDT:PSSH/PNDI/Al and d) ITO/PEDT:PSSH/PEIE/PNDI/Al devices. Sweep cycle: $0 \rightarrow +8 \rightarrow -8 \rightarrow 0$ V (applied on Al; cycle time, 5 s). Energy-level alignment diagram is shown in inset. Bias preconditioning: e) (Top) Current density before and after bias preconditioning of ITO/PEDT:PSSH/PEIE/PNDI/Al devices. Bias level: ±8 V; duration, 2.5 s. Probe-pulse voltage: ±8 V; duration, 130 ms. (Bottom) Microscope images of device taken through the ITO side before and after JV sweeps. Size of image, 1×1 mm.

to PNDI, as revealed by the classic space-charge-limited current densities (SCLC) behaviur, $J \propto (V - V_{bi})^2 d^{-3}$, for $-8 \lesssim V \lesssim -3$, where d is the OSC film thickness (see Figure S2 in the Supporting Information). We found an electron SCLC mobility for PNDI of 1.1×10^{-4} cm^2 V^{-1} s^{-1}, which is slightly lower than that reported earlier (5×10^{-4} cm^2 V^{-1} s^{-1}), possibly due to differences in processing.[25] Electron injection from PEDT:PSSH/PEIE in the first sweep, however, is at least two orders of magnitude lower than Al. This confirms previous reports that the PEIE interlayer does not by itself provide electron injection in electron-only diodes.[11,14]

However, while the injection from Al is stable with repeated sweeps, the injection from PEDT:PSSH/PEIE improves quickly with repeated JV cycling, eventually reaching that of Al. To clearly demonstrate the bias polarity dependence of this phenomenon, we apply a 130 ms probe pulse of -8 or $+8$ V to the diode ("before"), followed by a 2500 ms constant bias at -8 or $+8$ V (all voltages on Al), and then the same 130 ms probe pulse ("after") in separate experiments on new devices. The J values of the probe pulses are displayed in Figure 2e. J increases only for electron injection from PEDT:PSSH/PEIE, and only after positive-bias preconditioning of the PEDT:PSSH/PEIE side. These observations suggest that positive bias on the PEIE/PNDI contact results in cumulative changes, which decline slightly in the rest state, and more when strongly negative biased (Figure S3, Supporting Information).

The PEIE/PNDI contact thus turns from electron-blocking to electron-injecting, with current density that matches that of Al at the same absolute bias. This is confirmed also by capacitance measurements at zero V_{dc}. The PEDT:PSSH/PNDI/Al diode has a capacitance of 1.0 nF, frequency independent over 1–100 kHz, corresponding to the geometric capacitance of the PNDI film

($\varepsilon_r \approx 3.2$; Figure S4, Supporting Information). When the PEIE monolayer is inserted, V_{bi} downshifts to zero V, and the capacitance becomes 14 nF at 1 kHz (and 2.0 nF at 100 kHz) without bias-conditioning, due to the diffusion capacitance of electrons injected by Al. After bias-conditioning, the capacitance doubles to 30 nF at 1 kHz (4 nF at 100 kHz), consistent with contribution from additional diffusion capacitance due to electrons injected by PEDT:PSSH/PEIE in the other half cycle.

Spectroscopy confirms that the initial doping level at the PNDI interface becomes amplified by the positive bias, where the emergent yellow coloration can be visually observed (bottom panel, Figure 2e). We performed comparative in-device Raman spectroscopy on ITO/PEIE/PNDI/Al and ITO/PNDI/Al devices (**Figure 3**a). The ITO/PEIE/PNDI/Al device gives similar characteristics as the ITO/PEDT:PSSH/PEIE/PNDI/Al device, but avoids the strong Raman features of PEDT:PSSH and their marked bias dependence.[23] The spectra of a pristine PNDI film, and an electron-doped one (1.0 e^-/repeat unit), made by contacting the pristine film with a cobaltocene solution,[8] are shown for reference. Electron doping produces a characteristic strong band at 1539 cm^{-1}, and a weak band at 1660 cm^{-1}. PEIE exhibits only weak Raman features below 1500 cm^{-1}, buried by PNDI features, while ITO–glass has no features in this spectral range. The starting PNDI film is already slightly electron-doped, because of the low work function of ITO/PEIE, and also Coulombic disorder-induced doping.[31] The accumulation electron density is limited by the relatively small capacitance of the PEIE tunnel barrier.[15] When the PEIE/PNDI junction is positive biased, however, a marked increase in electron doping level occurs (by a factor of 5–8) within few seconds before leveling off. This does not occur in the absence of the PEIE monolayer, even after 6 h of continuous positive bias, providing unequivocal
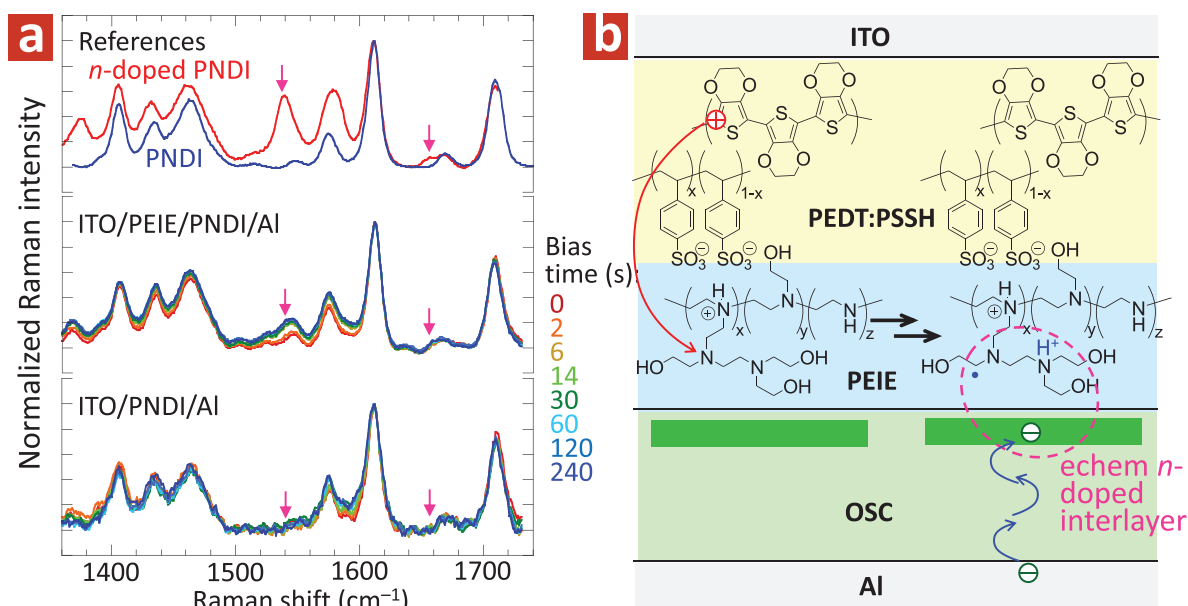
Figure 3. In-device Raman spectroscopy and formation of bias-induced electrochemical n-doped interlayer. a) (Top) Raman spectra of PNDI and electron-doped PNDI films (1.0 e^-/repeat unit), normalized to peak intensity at 1612 cm^{-1} for reference. Thickness, 100 nm. (Middle) Raman spectra of ITO/PEIE/PNDI/Al device and (bottom) ITO/PNDI/Al device, both as a function of cumulative bias time shown in legend (-8 V on Al). b) Schematic mechanism for the bias-induced electrochemical electron-doping of the OSC interface associated with amine oxidation of PEIE.

evidence for electrochemical electron doping of the PNDI interface with PEIE when the PEIE side is positively biased.

A schematic of this interfacial, solid-state in-device electrochemical doping mechanism is shown in Figure 3b. Strong positive bias of the PEIE side injects holes into the amine nitrogens to form tertiary aminium sites, which rearrange by α proton transfer to give stable protonated ammonium sites.[32] This is accompanied by electron injection from the opposite contact to give a δ-doped layer at the semiconductor interface with PEIE, stabilized by the electric field effect, producing a persistent electron-doped interface. This resembles the ability of a polyelectrolyte counter-ion monolayer to stabilize a doped semiconductor interface,[31] except that the counter-ion monolayer here is produced in situ by electrical injection. Fundamentally, it is an electrochemical process that occurs without supporting electrolyte, different from light-emitting electrochemical cells.[33] As a consequence, the electrical doping is advantageously confined to the interface. This adds a new mechanism to emerging facets of in-device electrochemistry previously found in PEDT:PSSH and S-P3MEET:PHOST, where electrical injection into the conducting polymer results in overdoping/dedoping, causing conductivity fading, when accompanied by sulfonic acid Faradaic processes.[4,23,34] The build-up of carrier density appears to negate resistance of the PSSH:PEIE tunnel barrier (4 nm) formed at the PEDT:PSSH/PEIE/PNDI contact. One reason may be mitigation by the higher hopping density of carrier sites in the current detailed balance model.[2]

To confirm its generality, we examined the bias-conditioning systematics for another OSC, poly(2,5-bis(alkyl)-1,4-dioxopyrrolo[3,4-*c*]pyrrole-3,6-diyl-thiophene-2,5-diylthieno[2,3-*b*]thiophene-2,5-diyl-thiophene-2,5-diyl) (DPP). DPP has $E_A \approx 0.5$ eV lower than PNDI, hence LUMO band edge further upenergy from the FL of PEDT:PSSH. As a result, the PEDT:PSSH/DPP/Al diode is hole dominated (Figure S5, Supporting Information). Preconditioning in any polarity does not change injection in either polarity. Assembly of PEIE monolayer to give the PEDT:PSSH/PEIE/DPP/Al diode shuts down the hole current, leaving the electron current. Applying a positive bias on the PEDT:PSSH/PEIE side increases the electron current from that contact to approach that from Al, although this cannot be expected to reach the ohmic regime because of the large thermodynamic barrier that remains. Applying a positive bias on the Al side does not change any current. Replacing the Al contact with Pd decreases electron current from that contact slightly, but positive bias on PEDT:PSSH/PEIE still increases its subsequent electron current. Improvement is also observed for poly(9,9-bis(4-octylphenyl)fluorene-2,7-diyl) (PFOP) as OSC (Figure S6, Supporting Information).

In summary, we have demonstrated a new in-device electrochemical mechanism that can charge dope the interface of an organic semiconductor with an appropriate material that can undergo the complementary Faradaic process to generate stable ion of opposite charge sign by bias preconditioning. The in situ electrochemistry is more pervasive than previously thought,[4,23,35] and can under some circumstances be exploited to generate the desired ohmic contact at internal interfaces. This allows the unprecedented ohmic electron injection from PEDT:PSSH into an organic semiconductor with $E_A \approx 3.9$ eV through a δ-doped layer induced by the positively charged PEIE monolayer that could be useful for tandem solar cells for example.

Experimental Section

Material and Film Preparation: PNDI was obtained from 1-Material Inc. and used as received. PFOP was obtained from Cambridge Display Technology, a subsidiary of Sumitomo Chemical Company (Japan), and used as received. DPP was synthesized in-house by the group of Prof L. L. Chua. ITO and Si(100)/Au substrates were cleaned with acetone and isopropyl alcohol (IPA), and then O$_2$ plasma or Standard-Clean 1. A commercial 1:6 wt/wt% PEDT:PSSH solution (Clevios P VP Al 4083, Heraeus Precious Metals GmbH) was purified by dialysis against 1-M semiconductor-grade HCl solution followed by Millipore water through a 12 kDa molecular-weight-cutoff membrane to remove metallic ions and other acid impurities. A 50 nm thick film was spin-cast and annealed in air at 150 °C (hotplate) for 10 min. For PEDT:PSSH/PEIE films, 35–40 wt% PEIE (Sigma-Aldrich) was diluted with 2-methoxyethanol to 0.4 wt% and spin-cast onto preformed PEDT:PSSH films (5000 rpm, 60 s). For ITO/PEIE films, this solution was spin-cast onto clean ITO (5000 rpm, 60 s). Unbounded PEIE was subsequently removed by spin-rinse with 2-methoxyethanol (30 s contact, then 5000 rpm spin-off). The substrates were then annealed in air (hotplate: 100 °C, 10 min). ITO or PEDT:PSSH films without PEIE were fabricated for comparison by omitting the PEIE steps. For electron-doped PNDI film, an undoped PNDI film was baked at 140 °C, 10 min, in a N$_2$ glovebox, and contacted with cobaltocene in acetonitrile for 10 s, and then spun off at high speed.

UPS and XPS Spectroscopies: UPS and XPS were performed on films in sequence in an ESCALAB UHV chamber equipped with an Omicron EA 125 U7 hemispherical electron energy analyser at a base pressure of 10^{-9} mbar. UPS was excited using He I radiation (21.21 eV) with minimal He II contamination. XPS was excited using MgKα X-rays (1253.6 eV). The photoemission normal to the film surface was collected, and analyzed at a resolution of 50 meV at pass energy of 5.0 eV for UPS, and a resolution of 0.7 eV with pass energy of 20 eV for XPS.

Fabrication of Diodes: PEDT:PSSH and PEDT:PSSH/PEIE films were fabricated on clean ITO as described above. PNDI (*p*-xylene solution), DPP (chlorobenzene solution), or PFOP (toluene solution) was spin-cast in the N$_2$ glovebox to give films of thicknesses 120, 80, and 80 nm, respectively. The film stack was then annealed in the glovebox (hotplate: 100 °C for PNDI, 120 °C for DPP and PFOP; 10 min). A 100 nm thick Al, or 40 nm thick Pd layer capped with Al, was thermally evaporated through a shadow mask at a base pressure of 10^{-7} mbar to give evaporated top electrode to define eight 4.3 mm^2 pixels on each substrate. The current–voltage characteristics were collected on a probe station in the N$_2$ glovebox using a Keithley 4200 semiconductor parameter analyzer.

Electroabsorption Spectroscopy: Electroabsorption spectroscopy measurements of the diodes were performed at 30 K in a closed-cycle He cryostat (Janis APD HC-2) at a base pressure of 10^{-6} mbar. A sinusoidal drive voltage superposed on the selected dc bias was injected into the diode. Monochromatic light was incident through the glass substrate at 45°, and its reflection off the cathode was collected by mirror optics onto a photodiode. The photocurrent was amplified by a gain of 10^6 and demodulated by a lock-in amplifier at 1 ω, phase locked to V_{ac} oscillation to give the induced change in absorbance as a function of wavelength.

Raman Spectroscopy: Raman spectra were collected using a Renishaw Raman microscope in the back-scattered geometry through ITO. Reference films were cast on glass and encapsulated in N$_2$. Argon ion laser (514 nm) was focused through an objective lens (numerical aperture 0.4; 20×).

Supporting Information

Supporting Information is available from the Wiley Online Library or from the author.

[1] M. Zhou, L. L. Chua, R. Q. Png, C. K. Yong, S. Sivaramakrishnan, P. J. Chia, A. T. S. Wee, R. H. Friend, P. K. H. Ho, *Phys. Rev. Lett.* **2009**, *103*, 036601.

[2] J. K. Tan, R. Q. Png, C. Zhao, P. K. H. Ho, *Nat. Commun.* **2018**, *9*, 3269.

[3] L. B. Groenendaal, F. Jonas, D. Freitag, H. Pielartzik, J. R. Reynolds, *Adv. Mater.* **2000**, *12*, 481.

[4] D. Belaineh, R. Q. Png, C. L. McGuiness, M. Mathai, V. Seshadri, P. K. H. Ho, *Chem. Mater.* **2014**, *26*, 4724.

[5] D. M. de Leeuw, M. M. J. Simenon, A. R. Brown, R. E. F. Einerhand, *Synth. Met.* **1997**, *87*, 53.

[6] a) B. Lüssem, M. Riede, K. Leo, *Phys. Status Solidi A* **2013**, *210*, 9; b) P. Wei, J. H. Oh, G. Dong, Z. Bao, *J. Am. Chem. Soc.* **2010**, *132*, 8852; c) S. Guo, S. B. Kim, S. K. Mohapatra, Y. Qi, T. Sajoto, A. Kahn, S. R. Marder, S. Barlow, *Adv. Mater.* **2012**, *24*, 699; d) X. Lin, B. Wegner, K. M. Lee, M. A. Fusella, F. Zhang, K. Moudgil, B. P. Rand, S. Barlow, S. R. Marder, N. Koch, A. Kahn, *Nat. Mater.* **2017**, *16*, 1209.

[7] C. G. Tang, M. Nur Syafiqah, Q. M. Koh, C. Zhao, J. Zaini, Q. J. Seah, M. J. Cass, M. J. Humphries, I. Grizzi, J. H. Burroughes, R. Q. Png, L. L. Chua, P. K. H. Ho, *Nature*, in press.

[8] C. G. Tang, M. C. Y. Ang, K. K. Choo, V. Keerthi, J. K. Tan, M. Nur Syafiqah, T. Kugler, J. H. Burroughes, R. Q. Png, L. L. Chua, P. K. H. Ho, *Nature* **2016**, *539*, 536.

[9] B. R. Lee, E. D. Jung, Y. S. Nam, M. Jung, J. S. Park, S. Lee, H. Choi, S. J. Ko, N. R. Shin, Y. K. Kim, S. O. Kim, J. Y. Kim, H. J. Shin, S. Cho, M. H. Song, *Adv. Mater.* **2014**, *26*, 494.

[10] Y. H. Zhou, C. Fuentes-Hernandez, J. W. Shim, J. Meyer, A. J. Giordano, H. Li, P. Wingte, T. Papadopoulos, H. Cheun, J. B. Kim, M. Fenoll, A. Dindar, W. Haske, E. Najafabadl, T. M. Khan, H. Sojoudi, S. Barlow, S. Graham, J. L. Brédas, S. R. Marder, A. Kahn, B. Kippelen, *Science* **2012**, *336*, 327.

[11] M. Takada, T. Nagase, T. Kobayashi, H. Naito, *Org. Electron.* **2017**, *50*, 290.

[12] P. K. H. Ho, M. Granström, R. H. Friend, N. C. Greenham, *Adv. Mater.* **1998**, *10*, 769.

[13] P. K. H. Ho, J. S. Kim, J. H. Burroughes, H. Becker, S. F. Y. Li, T. M. Brown, F. Cacialli, R. H. Friend, *Nature* **2000**, *404*, 481.

[14] Y. H. Kim, T. H. Han, H. Cho, S. Y. Min, C. L. Lee, T. W. Lee, *Adv. Funct. Mater.* **2014**, *24*, 3808.

[15] D. Belaineh, J. K. Tan, R. Q. Png, P. F. Dee, Y. M. Lee, B. N. N. Thi, N. S. Ridzuan, P. K. H. Ho, *Adv. Funct. Mater.* **2015**, *25*, 5504.

[16] a) H. Kang, S. Hong, J. Lee, K. Lee, *Adv. Mater.* **2012**, *24*, 3005; b) A. K. Kyaw, D. H. Wang, V. Gupta, J. Zhang, S. Chand, G. C. Bazan, A. J. Heeger, *Adv. Mater.* **2013**, *25*, 2397; c) V. A. Kolesov, C. Fuentes-Hernandez, W. F. Chou, N. Aizawa, F. A. Larrain, M. Wang, A. Perrotta, S. Choi, S. Graham, G. C. Bazan, T. Q. Nguyen, S. R. Marder, B. Kippelen, *Nat. Mater.* **2017**, *16*, 474.

[17] a) Y. Matsunaga, K. Goto, K. Kubono, K. Sako, T. Shinmyozu, *Chem. - Eur. J.* **2014**, *20*, 7309; b) S. Dadashi-Silab, S. Doran, Y. Yagci, *Chem. Rev.* **2016**, *116*, 10212.

[18] S. Höfle, A. Schienle, M. Bruns, U. Lemmer, A. Colsmann, *Adv. Mater.* **2014**, *26*, 2750.

[19] S. Ohisa, T. Kato, T. Takahashi, M. Suzuki, Y. Hayashi, T. Koganezawa, C. R. McNeill, T. Chiba, Y. J. Pu, J. Kido, *ACS Appl. Mater. Interfaces* **2018**, *10*, 17318.

[20] S. Fabiano, S. Braun, X. Liu, E. Weverberghs, P. Gerbaux, M. Fahlman, M. Berggren, X. Crispin, *Adv. Mater.* **2014**, *26*, 6000.

[21] B. Sun, W. Hong, E. S. Thibau, H. Aziz, Z. H. Lu, Y. Li, *ACS Appl. Mater. Interfaces* **2015**, *7*, 18662.

[22] L. L. Chua, P. K. H. Ho, H. Sirringhaus, R. H. Friend, *Appl. Phys. Lett.* **2004**, *84*, 3400.

[23] P. J. Chia, L. L. Chua, S. Sivaramakrishnan, J. M. Zhuo, L. H. Zhao, W. S. Sim, Y. C. Yeo, P. K. H. Ho, *Adv. Mater.* **2007**, *19*, 4202.

[24] H. Yan, Z. Chen, Y. Zheng, C. Newman, J. R. Quinn, F. Dötz, M. Kastler, A. Facchetti, *Nature* **2009**, *457*, 679.

[25] G. A. H. Wetzelaer, M. Kuik, Y. Olivier, V. Lemaur, J. Cornil, S. Fabiano, M. A. Loi, P. W. M. Blom, *Phys. Rev. B* **2012**, *86*, 165203.

[26] M. Zhou, R. Q. Png, S. H. Khong, S. Sivaramakrishnan, L. H. Zhao, L. L. Chua, R. H. Friend, P. K. H. Ho, *Appl. Phys. Lett.* **2012**, *101*, 013501.

[27] A. Kahn, *Mater. Horiz.* **2016**, *3*, 7.

[28] Q. Bao, X. Liu, S. Braun, J. Yang, Y. Li, J. Tang, C. Duan, M. Fahlman, *ACS Appl. Mater. Interfaces* **2018**, *10*, 6491.

[29] a) D. Poplavskyy, J. Nelson, D. D. C. Bradley, *Appl. Phys. Lett.* **2003**, *83*, 707; b) T. V. Woudenbergh, J. Wilderman, P. W. M. Blom, J. J. A. M. Bastiaansen, B. M. W. Langeveld-Voss, *Adv. Funct. Mater.* **2004**, *14*, 677; c) H. T. Nicolai, G. A. H. Wetzelaer, M. Kuik, A. J. Kronemeijer, B. de Boer, P. W. M. Blom, *Appl. Phys. Lett.* **2010**, *96*, 172107.

[30] R. Steyrleuthner, M. Schubert, F. Jaiser, J. C. Blakesley, Z. Chen, A. Facchetti, D. Neher, *Adv. Mater.* **2010**, *22*, 2799.

[31] W. L. Seah, C. G. Tang, R. Q. Png, V. Keerthi, C. Zhao, H. Guo, J. G. Yang, M. Zhou, P. K. H. Ho, L. L. Chua, *Adv. Funct. Mater.* **2017**, *27*, 1606291.

[32] A. Adenier, M. M. Chehimi, I. Gallardo, J. Pinson, N. Vilà, *Langmuir* **2004**, *20*, 8243.

[33] a) D. Ofer, R. M. Crooks, M. S. Wrighton, *J. Am. Chem. Soc.* **1990**, *112*, 7869; b) J. C. de Mello, N. Tessler, S. C. Graham, R. H. Friend, *Phys. Rev. B* **1998**, *57*, 12951.

[34] P. J. Chia, Y. C. Yeo, J. H. Burroughes, R. H. Friend, P. K. H. Ho, *Appl. Phys. Lett.* **2008**, *93*, 033314.

[35] J. S. Kim, P. K. H. Ho, C. E. Murphy, A. J. A. B. Seeley, I. Grizzi, J. H. Burroughes, R. H. Friend, *Phys. Chem. Lett.* **2004**, *386*, 2.